Acta Crystallographica Section D
Biological Crystallography
ISSN 0907-4449

Metal binding to porcine pancreatic elastase: calcium or not calcium

Manfred S. Weiss,* Santosh Panjikar, Elzbieta Nowak and Paul A. Tucker

EMBL Hamburg Outstation, c/o DESY, Notkestrasse 85, D-22603 Hamburg, Germany

Correspondence e-mail: msweiss@embl-hamburg.de

Received 1 May 02
Accepted 17 June 2002

PDB References: PPE, sodium citrate/$CaCl_2$ form, 1lka, r1lkasf; PPE, Na_2SO_4 form, 1lkb, r1lkbsf.

Porcine pancreatic elastase has been crystallized at slightly acidic pH under two similar but slightly different conditions. Diffraction data were collected at a wavelength of 1.5 Å to a maximum resolution of 1.7 Å. Both difference electron-density maps and anomalous difference electron-density maps suggest that in crystals grown from a sodium sulfate solution PPE binds Na^+ in its metal-binding site. In contrast, PPE binds Ca^{2+} in crystals grown from a solution containing sodium citrate and calcium chloride. This observation is in contradiction to most PPE structures reported in the PDB. In addition to the metal-binding site, up to three other binding sites, which appear to be anion-binding sites, could be identified based on the observed anomalous intensity differences.

1. Introduction

Porcine pancreatic elastase (EC 3.4.21.36) (PPE) is a serine protease homologous to trypsin and chymotrypsin (Hartley & Shotton, 1971). It consists of 240 amino acids cross-linked by four disulfide bridges and has been observed to bind to Ca^{2+} with a dissociation constant of $4.5 \times 10^{-5}\,M$ (Dimicoli & Bieth, 1977). PPE can be crystallized easily and is therefore used in many laboratories as a teaching example and a test case to investigate various crystallographic issues.

On February 20, 2002, there were 42 entries for PPE in its canonical space group $P2_12_12_1$ in the PDB (Berman *et al.*, 2000). All of these appear to have been crystallized from a solution containing both sodium and sulfate. In 33 of these cases (PDB codes 1bma, 1btu, 1e34, 1e35, 1e36, 1e37, 1e38, 1ela, 1elb, 1elc, 1eld, 1ele, 1elf, 1elg, 1esb, 1h9l, 1hax, 1hay, 1haz, 1hb0, 1inc, 1lvy, 1nes, 1qgf, 1qix, 1qr3, 3est, 4est, 5est, 6est, 7est, 8est and 9est), the authors report that the metal-binding site is occupied by a calcium ion. Only in four cases was the metal reported to be sodium (PDB codes 1eas, 1eat, 1eau and 1qnj); in five other cases, no metal was reported to be present in the binding site (PDB codes 1est, 1fzz, 1hv7, 1jim and 2est).

In order to resolve this apparent discrepancy, we have crystallized PPE from a sodium sulfate solution as well as from a sulfate-free solution containing sodium citrate and calcium chloride (Gilliland *et al.*, 1994). Based on the bond lengths to their neighbouring O atoms it is difficult to differentiate Na^+ and Ca^{2+} (Harding, 1999, 2002), but with ten and 18 electrons, the two ions should appear differently in electron-density maps. However, occupancy values differing from 1.0 as well as variations in the atomic temperature factor may effectively mask this difference. Faced with a similar problem, Einspahr *et al.* (1985) managed to distinguish Mn^{2+} from Ca^{2+} in a crystal of pea lectin based on the anomalous intensity differences

Table 1
$\Delta f''$ values at $\lambda = 1.5$ Å.

Element	$\Delta f''$† (e)
Ca	1.23
S	0.53
Na	0.12
O	0.03

† The values for $\Delta f''$ are based upon the theoretical approximation developed by Cromer & Liberman (1970). They were retrieved from the internet site of the Biomolecular Structure Center at the University of Washington, Seattle, USA (http://www.bmsc.washington.edu/scatter/AS_periodic.html).

observed at the absorption edge of manganese at $\lambda = 1.896$ Å. In their case, the difference in $\Delta f''$ values between Mn^{2+} and Ca^{2+} was 2.2 e, which is about twice as large as the difference between Na^+ and Ca^{2+} at $\lambda = 1.5$ Å (Table 1). Nevertheless, the fact that $\Delta f''$ of Na^+ is almost negligible and that the ten S atoms present in the PPE structure may be used as an internal standard for the magnitude of the signal encouraged us to proceed along this direction.

Based on highly redundant and therefore very accurate diffraction data sets from both PPE crystals, we are able to provide convincing evidence that PPE crystals grown from a sodium sulfate solution do not contain calcium, but contain sodium instead. If PPE crystals are grown from a solution containing a millimolar concentration of Ca^{2+} ions, however, the PPE metal-binding site is occupied by Ca^{2+} as expected.

In the light of the fact that PPE crystals are often used as test cases (also in our laboratory), it is necessary to know with as much certainty as possible what elements are present in the crystal and bound to the protein. In this respect, our findings may prove to be of wider interest.

2. Materials and methods

Commercially available porcine pancreatic elastase (Serva, Product No. 20929, Lot No. 13368) was used for crystallization without further purification. The protein material was dissolved in deionized water to concentrations of 12 or 20 mg ml^{-1}. For crystallization of the Na_2SO_4 crystal form, a 1 µl drop of protein solution ($c = 20$ mg ml^{-1}) was mixed with an equal volume of reservoir solution containing 100 m*M* sodium acetate buffer at pH 5.1 and 200 m*M* Na_2SO_4. The hanging drop was then equilibrated against this reservoir at room temperature. Crystal growth occurred within 1 or 2 d.

For crystallization of the sodium citrate/$CaCl_2$ form, a 1 µl drop of protein solution ($c = 12$ mg ml^{-1}) was mixed with an equal volume of reservoir solution containing 100 m*M* sodium acetate buffer at pH 5.1, 50 m*M* sodium citrate and 5 m*M* $CaCl_2$. The hanging drop was first incubated overnight at 298 K and then stored at room temperature. Crystal growth also occurred within 1 or 2 d.

For data collection, both crystals were flash-cooled in a nitrogen stream using dried paraffin oil as a cryoprotectant (Riboldi-Tunnicliffe & Hilgenfeld, 1999). Complete and highly redundant data sets were collected from both crystal forms at EMBL beamline X31 (DESY Hamburg) at a wavelength of 1.5 Å to a maximum resolution of 1.7 Å. For time and apparative reasons, we limited the maximum resolution for this experiment to 1.7 Å, although this was by no means the actual diffraction limit of the crystals. The data were processed using the program *DENZO* (Otwinowski, 1993) and scaled and merged using *SCALEPACK* (Otwinowski, 1993). Intensities were converted to structure factors using the method of French & Wilson (1978) as implemented in the program *TRUNCATE* (Collaborative Computational Project, Number 4, 1994). By applying the *TRUNCATE* procedure, the observed structure-factor amplitudes were also placed on an approximate absolute scale.

As a starting structure for refinement, the PDB entry 1qnj (resolution 1.1 Å, *R* factor = 12.7%; Würtele *et al.*, 2000) was used. All ions and solvent molecules were deleted from the

Table 2
Data collection and refinement statistics.

Values in parentheses are for the outer resolution shell. The resolution limits of this shell are 1.73–1.70 Å for both data sets.

	Na_2SO_4 form	Sodium citrate/$CaCl_2$ form
Data collection		
No. of crystals	1	1
Total rotation range (°)	500	405
Space group	$P2_12_12_1$	$P2_12_12_1$
Unit-cell parameters		
a (Å)	50.17	50.14
b (Å)	58.06	58.11
c (Å)	74.34	74.28
Resolution limits (Å)	99.0–1.70	99.0–1.70
Mosaicity (Å)	0.45	0.27
Total No. of reflections	466785	386243
Unique reflections	24415	24469
Redundancy	19.12	15.78
Completeness (%)	99.5 (99.0)	99.7 (100.0)
$I/\sigma(I)$	56.3 (18.6)	31.8 (19.9)
R_{merge}† (%)	5.3 (17.1)	8.5 (15.0)
$R_{r.i.m.}$‡ (%)	5.5 (17.6)	8.8 (15.5)
$R_{p.i.m.}$§ (%)	1.2 (4.1)	2.2 (3.9)
R_{anom} (%)	1.3 (3.8)	2.3 (4.3)
Overall *B* factor from Wilson plot (Å^2)	13.4	12.6
Optical resolution¶ (Å)	1.32	1.31
Refinement		
Resolution limits (Å)	40.0–1.70	40.0–1.70
Data cutoff [$F/\sigma(F)$]	0.0	0.0
Total No. of reflections	24415	24468
No. of reflections in working set	23164	23214
No. of reflections in test set	1251	1254
R (%)	16.93	16.89
R_{free} (%)	20.34	21.60
No. of amino-acid residues	240	240
No. of protein atoms††	1845	1845
No. of ion atoms	12‡‡	6§§
No. of solvent atoms	288	292
R.m.s.d. bond lengths (Å)	0.010	0.010
R.m.s.d. bond angles (°)	2.1	2.1

† $R_{merge} = \sum_{hkl}\sum_i |I_i(hkl) - \overline{I(hkl)}|/\sum_{hkl}\sum_i I_i(hkl)$, where $\sum_{hkl}$ denotes the sum over all reflections and $\sum_i$ the sum over all equivalent and symmetry-related reflections. ‡ $R_{r.i.m.}$ is the redundancy-independent merging *R* factor (Weiss, 2001). $R_{r.i.m.} = \sum_{hkl}[N/(N-1)]^{1/2}\sum_i |I_i(hkl) - \overline{I(hkl)}|/\sum_{hkl}\sum_i I_i(hkl)$, with *N* being the number of times a given reflection has been observed. § $R_{p.i.m.}$ is the precision-indicating merging *R* factor (Weiss, 2001). $R_{p.i.m.} = \sum_{hkl}[1/(N-1)]^{1/2}\sum_i |I_i(hkl) - \overline{I(hkl)}|/\sum_{hkl}\sum_i I_i(hkl)$. ¶ According to Vaguine *et al.* (1999). †† The side chains of Tyr82, Val168, Gln199 and Arg211 have been modelled in two conformations. ‡‡ One Na^+, one Cl^- and two SO_4^{2-}. §§ One Ca^{2+}, one Cl^- and one CH_3COO^-.

model, multiple conformations were reduced to the major conformation and all atomic temperature factors were set to be equal. After rigid-body refinement and restrained refinement of the protein atoms only, the anomalous difference electron density as well as the (F_{obs} − F_{calc}) difference electron-density maps and the [F_{obs}(Ca) − F_{obs}(Na)] difference electron-density maps were computed. Further refinement included the addition of ions and solvent molecules as well as manual inspection of the model using computer graphics. All refinement and electron-density map calculations were performed using programs from the *CCP*4 suite (Collaborative Computational Project, Number 4, 1994).

3. Results and discussion

Some details of data collection and processing are given in Table 2. From the numbers, it is evident that both collected data sets are of very high quality. The values obtained for the optical resolution corroborate the notion that the actual diffraction limit of the crystals used was actually much higher than 1.7 Å, as pointed out previously in §2. In the case of the Na_2SO_4 crystal form, the b* axis was oriented almost parallel to the spindle axis. This precluded the achievement of a

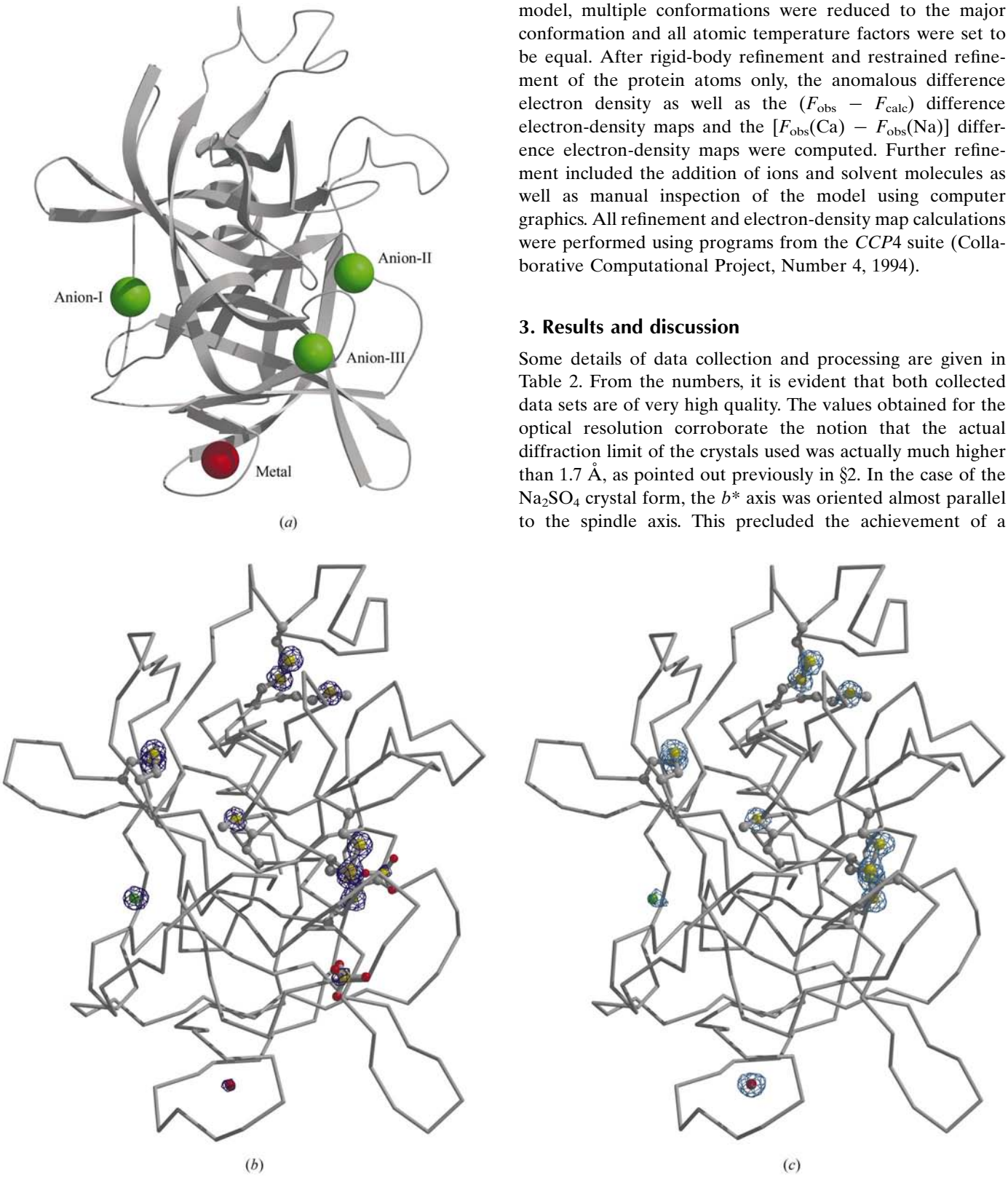

Figure 1
(*a*) Schematic view of the structure of PPE with the different binding sites pointed out. The active site is located close to the anion-II site; (*b*) C^{α} trace of PPE in the Na_2SO_4 form with the 13 highest peaks plus the peak at the metal-binding site (No. 15) of the anomalous difference electron-density map displayed in blue; (*c*) C^{α} trace of PPE in the sodium citrate/$CaCl_2$ form with the 12 highest peaks of the anomalous difference electron density map displayed in cyan. In both cases the contour level of the electron-density map was 0.024 e Å^{-3}. The figure was prepared using the programs *BOBSCRIPT* (Esnouf, 1997) and *Raster3D* (Merritt & Bacon, 1997).

comparable completeness as for the sodium citrate/$CaCl_2$ form using rotation about just one axis. Therefore, after 300° of rotation the orientation was changed by about 10° and another 100° of data were collected to cover the blind region. The data set for the Na_2SO_4 crystal form appears to be of slightly higher quality based on the observed merging statistics (Table 2).

The anomalous differences as described by R_{anom} are very small in both cases as expected, but they are slightly larger than the errors in the merged intensities, as described by $R_{p.i.m.}$. This appears to be a good indicator of the quality of the anomalous differences (Weiss *et al.*, 2001; Panjikar & Tucker, 2002). It is also apparent that the sodium citrate/$CaCl_2$ data exhibits a larger anomalous signal than the Na_2SO_4 data.

In order to avoid any bias caused by the presence of solvent molecules or ions in the structures, the difference electron-density maps and the anomalous difference electron-density maps were calculated after rigid-body and restrained refinement of the protein atoms only. The R and R_{free} values at this stage were 26.3 and 30.7% for the Na_2SO_4 data and 26.1 and 30.3% for the sodium citrate/$CaCl_2$ data, respectively. Even though the difference in the $\Delta f''$ values for Na and Ca at the wavelength λ = 1.5 Å is only about 1.1 e (Table 1), the anomalous difference electron-density maps of the two data sets appear very different at the metal-binding site (Fig. 1). The absolute and relative heights as well as the ranks of the top peaks in the four maps are listed in Table 3. It is important to note that the anomalous difference electron-density maps have different root-mean-square (r.m.s.) values. Therefore, all peaks appear to be higher in the Na_2SO_4 case when viewed in units of r.m.s. If one considers the absolute peak heights, however, it becomes clear that this is not the case and that the peak heights for the S atoms are indeed of the same magnitude in both maps. From the lists of peaks in the various electron-density maps, it is evident that PPE contains a total of four major binding sites: a metal-binding site, an anion-binding site near Ser14 (anion-I), a second anion-binding site in the active site near Ser188 (anion-II) and a sulfate-binding site at a crystal contact between Arg136 and Arg225 of a symmetry-related molecule (anion-III) (Fig. 1).

Table 3
Heights and ranks of the difference-map peaks.

	Na_2SO_4 form			Sodium citrate/$CaCl_2$ form		
Atom	Height (r.m.s)	Height (e Å^{-3})	Rank	Height (r.m.s.)	Height (e Å^{-3})	Rank
$F_{obs} - F_{calc}$ maps†						
Metal site	10.9	0.91	2	14.7	1.28	1
Anion-I site‡	11.1	0.92	1	7.7	0.67	11
Anion-II site‡	8.3	0.70	7	5.0	0.44	99
Anion-III site‡	5.5	0.46	82	—	—	—
Other (water)	9.1	0.76	3	9.1	0.79	2
$F^+ - F^-$ maps†						
Metal site	5.7	0.034	15	17.1	0.178	1
Cys30 SG	18.0	0.108	5	11.3	0.118	7
Met41 SD	17.2	0.103	9	11.2	0.116	8
Cys46 SG	17.5	0.105	6	12.6	0.131	2
Cys127 SG	21.1	0.127	1	11.8	0.123	5
Cys158 SG	17.4	0.104	7	10.7	0.111	11
Met172 SD	16.9	0.101	10	12.1	0.126	4
Cys174 SG	19.6	0.118	2	11.1	0.115	9
Cys184 SG	17.3	0.104	8	10.9	0.113	10
Cys194 SG	19.0	0.114	4	11.5	0.120	6
Cys214 SG	19.5	0.117	3	12.1	0.126	3
Anion-I site‡	15.9	0.095	11	4.3	0.045	12
Anion-II site‡	6.9	0.041	12	—	—	—
Anion-III site‡	6.6	0.040	13	—	—	—
Next	6.0	0.036	14	4.3	0.045	13

† The absolute values for the maximum, the minimum and the root-mean-square deviation of the electron density for the four electron-density maps are as follows. ($F_{obs} - F_{calc}$) map of the Na_2SO_4 form: 0.92, −0.39 and 0.084 e Å^{-3}, respectively. ($F_{obs} - F_{calc}$) map of the sodium citrate/$CaCl_2$ form: 1.27, −0.36 and 0.087 e Å^{-3}, respectively. ($F^+ - F^-$) map of the Na_2SO_4 form: 0.126, −0.032 and 0.0060 e Å^{-3}, respectively. ($F^+ - F^-$) map of the sodium citrate/$CaCl_2$ form: 0.178, −0.045 and 0.0104 e Å^{-3}, respectively. ‡ The anion-I site is located near Ser14, the anion-II site in the active site of the enzyme near Ser188 and the anion-III site at a crystal contact between Arg136 and Arg225.

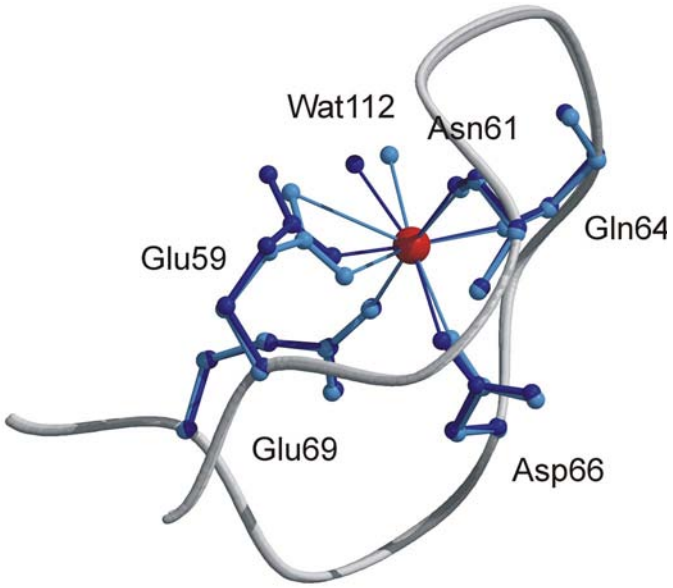

Figure 2
The metal-binding site of PPE. The metal site is shown in red, the traces of loop 58–70 in grey and the atoms of the amino acids and water molecules coordinating the metal in dark blue (Na_2SO_4 complex) and light blue (sodium citrate/$CaCl_2$ complex). The two structures were superimposed so that the metal coordinates are identical in both cases. This figure was also prepared using the programs *MOLSCRIPT* (Kraulis, 1991) and *Raster3D* (Merritt & Bacon, 1997).

3.1. The refined structures

As indicated by the refinement statistics (Table 2) both PPE structures are of very good quality. With R_{free} factors close to 20%, the structures can be considered to be well refined. The relatively large number of ordered water molecules reflects the precision and the quality of the data on the one hand, but may also be a consequence of the fact that hydrophobic paraffin oil is used as a cryoprotectant rather than a hydrophilic compound such as glycerol.

3.2. The metal-binding site

The metal bound to PPE is coordinated by amino-acid residues located on loop 59–69. The participating groups are the carboxylate groups of Glu59, Asp66 and Glu69 as well as

Table 4
Coordination distances of the metal ions in PPE.

Ligand atom	Na^+ in the Na_2SO_4 form (Å)	Ca^+ in the sodium citrate/$CaCl_2$ form† (Å)
Glu59 OE1	2.31	2.25 (eq)
Glu59 OE2	(3.78)	3.11 (eq)
Asn61 O	2.30	2.30 (ax)
Gln64 O	2.43	2.35 (eq)
Asp66 OD2	2.38	2.33 (eq)
Glu69 OE2	2.38	2.38 (ax)
Water 112	2.38	2.34 (eq)
Average‡	2.36	2.33

† Eq, equatorial ligand; ax, axial ligand of the pentagonal bipyramid. ‡ Based on six ligand-atom distances (not taking Glu59 OE2 into account). Expected average Me^{n+} distances are 2.42 Å for $Na^+\cdots O$ (Harding, 2002) and 2.38 and 2.39 Å for six- and seven-coordinated $Ca^{2+}\cdots O$, respectively (Harding, 1999).

the main-chain carbonyl O atoms of Asn61 and Gln64, and one water molecule. In the difference electron-density maps of the sodium citrate/$CaCl_2$ crystal form, the peak height at this site is significantly higher than anywhere else, whereas in the Na_2SO_4 crystal form it is about the same as for the water molecules. In the anomalous difference density maps of the Na_2SO_4 crystal form, the peak height at the metal site is only about one third of the height of the sulfur peaks, whereas in the sodium citrate/$CaCl_2$ crystal form it is again considerably higher. These observations suggest that PPE binds mainly Ca^{2+} in the sodium citrate/$CaCl_2$ crystal form and mainly Na^+ in the Na_2SO_4 case. Owing to the correlation between occupancy and temperature factor, it is difficult to estimate accurate occupancy values from these peak heights, but using the average sulfur peak height as internal standard and assuming that the metal site is in both cases occupied by a mixture of Na^+ and Ca^{2+}, the Na^+ occupancy in the Na_2SO_4 case is close to 100%, whereas the Ca^{2+} occupancy in the sodium citrate/$CaCl_2$ case is at least 60%. Taking the peak height of the strongest water molecule as a standard for the $(F_{obs} - F_{calc})$ difference maps, very similar values are obtained.

The coordination of the cation is almost ideally octahedral, allowing both ions to bind (Fig. 2). However, in the case of Ca^{2+} the second carboxylate O atom of Glu59 moves slightly towards the metal ion mainly by a rotation of the side chain around χ_2 by about 10°. This movement pushes the coordinating water molecule (Water 112) about 0.9 Å away from the carboxylate and distorts the octahedron somewhat in the direction of a pentagonal bipyramid, which is the preferred coordination geometry for Ca^{2+} (Harding, 1999). Overall, the ion-to-ligand atom distances (Table 4) are shorter for the Ca^{2+} case, which lends additional support to our interpretation.

The binding of the different metals does not cause any significant structural rearrangement in PPE. The r.m.s. deviation between the two structures based on all 240 C^α atoms is about 0.07 Å, which is clearly below the expected coordinate error. This observation is also in accord with the fact that neither the binding of Na^+ nor of Ca^{2+} has a major influence on the catalytic activity of the enzyme (Hartley & Shotton, 1971).

Our findings with respect to the identity of the metal ion are in contrast with most of the PPE structures in the PDB. In the first high-resolution structure of PPE in the PDB (PDB code 1est, resolution 2.5 Å; Sawyer *et al.*, 1978), the electron-density peak at the metal-binding site was interpreted as a water molecule because it was of similar strength to peaks for internal water molecules. However, the possibility of Ca^{2+} binding was mentioned. In later structures (PDB codes 1nes and 3est, resolution 1.65 Å; Meyer *et al.*, 1986, 1988), Ca^{2+} binding was reported, with a reference to Dimicoli & Bieth (1977), although the PPE crystals were grown under the same conditions. Since the 3est coordinates were used as starting structure in most subsequent PPE structure analyses, we suspect that the presence of Ca^{2+} in 3est led to the presence of Ca^{2+} in later PPE structures. Considering the thermodynamic equilibrium constants ($4.5 \times 10^{-5}\,M$ for the dissociation constant of the PPE–Ca^{2+} complex and $9.1 \times 10^{-6}\,M$ for the solubility product of $CaSO_4$), it appears unlikely that any Ca^{2+} can be left bound to PPE when sodium sulfate is used as a precipitant. We therefore believe that most of the PPE structures in the PDB need to be revised with respect to the identity of the bound metal ion.

3.3. The ion-binding site near Ser14

An unexpected feature was detected in the various anomalous and difference electron-density maps suggesting the presence of an ion near Ser14. The coordination is tetrahedral with the coordinating atoms being Ser14 OG, Ser14 N and two water molecules. Since this peak is almost spherical, we interpret it as a chloride ion. The presence of chloride in both cases can be explained by the fact that hydrochloric acid was used to adjust the pH of the acetate buffer. We have no explanation, however, of why this feature appears to be stronger in the Na_2SO_4 case than in the sodium citrate/$CaCl_2$ case.

3.4. The sulfate/acetate-binding site in the active site near Ser188

Another anion-binding site has been detected close to the active-site serine Ser188. In the Na_2SO_4 crystal form this anion is clearly a sulfate ion (although probably not 100% occupied), whereas in the sodium citrate/$CaCl_2$ form it is an acetate ion from the buffer. The two O atoms of the acetate assume almost identical positions to two of the O atoms of the sulfate ion.

3.5. The sulfate-binding site between Arg136 and Arg225

At a crystal contact a sulfate ion is bound to the Na_2SO_4 crystal form. This sulfate is of course not present in the sodium citrate/$CaCl_2$ crystal form.

4. Summary and conclusions

We have reported the crystal structures of porcine pancreatic elastase obtained from two similar but slightly different crystallization conditions. If PPE crystals are grown from a

Na_2SO_4-containing solution the metal-binding site of PPE is occupied by a sodium ion, whereas if PPE crystals are grown from a sodium citrate/$CaCl_2$-containing solution the metal-binding site of PPE contains mainly a calcium ion. The binding of the different metals is accompanied by only a slight rearrangement of the amino-acid residues building up the metal-binding site. Overall, the two structures are very similar. Three further binding sites have been identified in PPE: one chloride-binding site near Ser14, one sulfate/acetate-binding site in the active site and one sulfate-binding site between two Arg residues at a crystal contact.

In which respects our findings for PPE may be relevant to other metal-containing protein structures we do not know. It is clear, however, that great care must be taken to ensure that the bound metal is identified properly from the diffraction data and if necessary also by other means.

This work was partially supported by the EU 5th Framework RTD project (HPRI-1999-CT-50015) and by a European Community Marie Curie Fellowship (to EN).

References

Berman, H. M., Westbrook, J., Feng, Z., Gilliland, G., Bhat, T. N., Weissig, H., Shindyalov, I. N. & Bourne, P. E. (2000). *Nucleic Acids Res.* **28**, 235–242.
Collaborative Computational Project, Number 4 (1994). *Acta Cryst.* D**50**, 760–763.
Cromer, D. T. & Liberman, D. A. (1970). *J. Chem. Phys.* **53**, 1891–1898.
Dimicoli, J. L. & Bieth, J. (1977). *Biochemistry*, **16**, 5532–5537.
Einspahr, H., Suguna, K., Suddath, F. L., Ellis, G., Helliwell, J. R. & Papiz, M. Z. (1985). *Acta Cryst.* B**41**, 336–341.
Esnouf, R. M. (1997). *J. Mol. Graph.* **15**, 132–134.
French, G. S. & Wilson, K. S. (1978). *Acta Cryst.* A**34**, 517–525.
Gilliland, G. L., Tung, M., Blakeslee, D. M. & Ladner, J. (1994). *Acta Cryst.* D**50**, 408–413.
Harding, M. M. (1999). *Acta Cryst.* D**55**, 1432–1443.
Harding, M. M. (2002). *Acta Cryst.* D**58**, 872–874.
Hartley, B. S. & Shotton, D. M. (1971). *The Enzymes*, edited by P. D. Boyer, 3rd ed., Vol. III, pp. 323–373. New York: Academic Press.
Kraulis, P. J. (1991). *J. Appl. Cryst.* **24**, 946–950.
Merritt, A. E. & Bacon, D. J. (1997). *Methods Enzymol.* **277**, 505–524.
Meyer, E., Cole, G., Radhakrishnan, R. & Epp, O. (1988). *Acta Cryst.* B**44**, 26–38.
Meyer, E. F. Jr, Radhakrishnan, R., Cole, G. M. & Presta, L. G. (1986). *J. Mol. Biol.* **189**, 533–539.
Otwinowski, Z. (1993). *Proceedings of the CCP4 Study Weekend. Data Collection and Processing*, edited by L. Sawyer, N. Isaacs & S. Bailey, pp. 56–62. Warrington: Daresbury Laboratory.
Panjikar, S. & Tucker, P. (2002). *J. Appl. Cryst.* **35**, 261–266.
Riboldi-Tunnicliffe, A. & Hilgenfeld, R. (1999). *J. Appl. Cryst.* **32**, 1003–1005.
Sawyer, L., Shotton, D. M., Campbell, J. W., Wendell, P. L., Muirhead, H. & Watson, H. C. (1978). *J. Mol. Biol.* **118**, 137–208.
Vaguine, A. A., Richelle, J. & Wodak, S. J. (1999). *Acta Cryst.* D**55**, 191–205.
Weiss, M. S. (2001). *J. Appl. Cryst.* **34**, 130–135.
Weiss, M. S., Sicker, T. & Hilgenfeld, R. (2001). *Structure*, **9**, 771–777.
Würtele, M., Hahn, M., Hilpert, K. & Höhne, W. (2000). *Acta Cryst.* D**56**, 520–523.